Measurement of Carbon−Proton Dipolar Couplings in Liquid Crystals Using DAPT

S. Jayanthi,[†] P. K. Madhu,[‡] and K. V. Ramanathan*[,§]

Department of Physics, Indian Institute of Science, Bangalore, 560 012 India, Department of Chemical Sciences, Tata Institute of Fundamental Research, Homi Bhabha Road, Colaba, Mumbai. 400 005 India, and NMR Research Centre, Indian Institute of Science, Bangalore, 560 012 India

Received: May 29, 2008; Revised Manuscript Received: August 9, 2008

Dipolar couplings provide valuable information on order and dynamics in liquid crystals. For measuring heteronuclear dipolar couplings in oriented systems, a new separated local field experiment is presented here. The method is based on the dipolar assisted polarization transfer (DAPT) pulse sequence proposed recently (*Chem. Phys. Lett*. **2007**, *439*, 407) for transfer of polarization between two spins I and S. DAPT utilizes the evolution of magnetization of the I and S spins under two blocks of phase shifted BLEW-12 pulses on the I spin separated by a 90° pulse on the S spin. Compared to the rotating frame techniques based on Hartmann−Hahn match, this approach is easy to implement and is independent of any matching conditions. DAPT can be utilized either as a proton encoded local field (PELF) technique or as a separated local field (SLF) technique, which means that the heteronuclear dipolar coupling can be obtained by following either the evolution of the abundant spin like proton (PELF) or that of the rare spin such as carbon (SLF). We have demonstrated the use of DAPT both as a PELF and as a SLF technique on an oriented liquid crystalline sample at room temperature and also have compared its performance with PISEMA. We have also incorporated modifications to the original DAPT pulse sequence for (i) improving its sensitivity and (ii) removing carrier offset dependence.

I. Introduction

Two dimensional separated local field (SLF) NMR spectroscopy[1] is one of the most powerful and widely used NMR techniques to measure heteronuclear dipolar couplings. Since it provides site specific dipolar splittings for aligned samples, these experiments are extensively used for the study of biomolecules in lipid bilayers, liquid crystals or single crystals.[2] A majority of these experiments are based on the rotating frame Hartmann−Hahn match[3,4] and belong to a class of SLF experiments where ^{13}C or ^{15}N magnetization evolves under the local heteronuclear dipolar field in the indirect dimension.[5−11] There also exists another class of local field experiments named as proton encoded local field (PELF) spectroscopy[12−16] in which the ^{1}H magnetization evolves in the indirect dimension under the heteronuclear dipolar coupling. Pines and co-workers[13,14] demonstrated that this latter method has substantially improved resolution compared to the former. In the SLF experiment since each carbon is dipolar coupled to many protons, the resulting spectra may show a multiplet structure which can broaden the dipolar cross-peaks and also make the analysis difficult. On the other hand in the PELF scheme applied to unlabeled samples, each proton has only one relevant heteronuclear dipolar coupling and hence each pair of bonded carbon and proton gives rise to a single doublet with a large splitting. Long range couplings yield separate pairs of peaks with smaller splittings close to the center. Hence the PELF spectrum has a simple appearance and is easy to analyze. All of the pulse sequences mentioned above utilize Hartmann−Hahn cross polarization either for dipolar evolution or for polarization transfer.

In this paper we consider a new polarization transfer scheme named as DAPT[17] proposed recently for this purpose. DAPT is analogous to the INEPT sequence in liquids[18] and the PRESTO sequence for solid samples spinning at magic angle.[19] It employs the well-known homonuclear dipolar decoupling sequence BLEW-12[20] applied on the I spins and suitably phase shifted in two consecutive evolution periods together with a 90° pulse on the S spin in the middle. DAPT not only ensures a coherent transfer of magnetization between the spins I and S but also enables the measurement of the coupling between them. In this paper the pulse sequence proposed earlier has been modified to improve sensitivity and to refocus unwanted chemical shift evolutions of both I and S spins. We then examine the use of DAPT both as a PELF and as a SLF scheme. The experimental demonstration has been carried out on a sample of oriented chloroform and also on the liquid crystal *N*-(4-ethoxy benzylidine)-4-*n*-butylaniline (EBBA). The results obtained are compared with those obtained using the well-known PISEMA[5] sequence.

II. Improved DAPT Sequence

The pulse sequence proposed originally[17] is shown in Figure 1a. The sequence starts with a block of BLEW-12 pulses denoted as P_0 on the I spins applied for a time τ_1. This is followed by a 90° pulse with phase Y on the S spins. Subsequently a block of BLEW-12 pulses denoted as P_{90} is applied on the I spins for a time period τ_2. Pulses in the P_{90} block are phase shifted by 90° compared to those in the P_0 block. At the end of the τ_2 period, S spin signals are acquired under heteronuclear spin decoupling. It was shown earlier that this sequence referred to here as DAPT-I is able to achieve polarization transfer efficiently in static oriented systems. However there are two shortcomings in the above-mentioned sequence namely, (i) only 80% of the I spin polarization is

* To whom correspondence should be addressed. Fax: +91-80-23601550. E-mail: kvr@nrc.iisc.ernet.in.
† Department of Physics, Indian Institute of Science.
‡ Tata Institute of Fundamental Research.
§ NMR Research Centre, Indian Institute of Science.

10.1021/jp804764q CCC: $40.75
Published on Web 10/09/2008

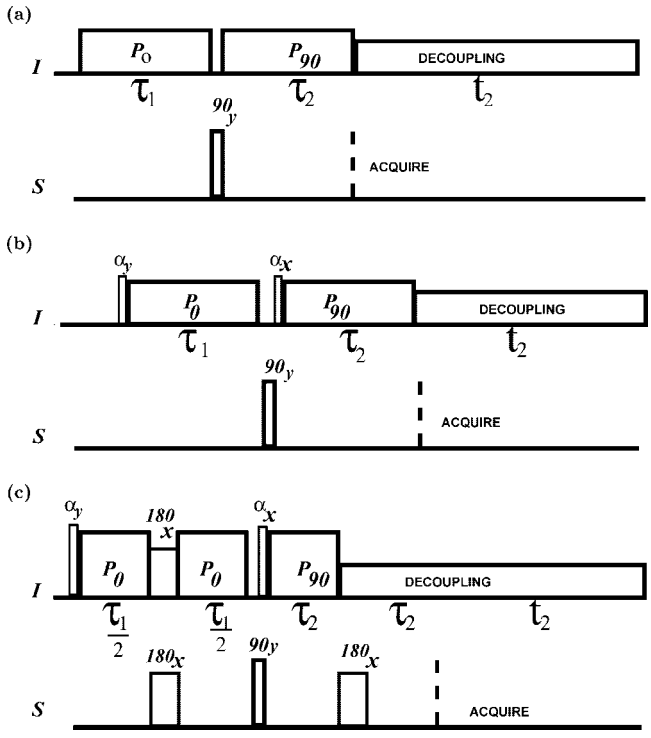

Figure 1. (a) DAPT-I pulse sequence as proposed originally.[17] P_0 and P_{90} denote blocks of BLEW-12 pulses applied during τ_1 and τ_2 respectively. Pulses applied during τ_2 have an additional phase shift of 90° compared to those applied during τ_1. (b) DAPT-II pulse sequence. Initial α° pulses improve the sensitivity by 25%. (c) DAPT-III pulse sequence. Along with sensitivity enhancement, simultaneous 180° pulses on both ^{13}C and ^{1}H refocus the chemical shift evolution of ^{1}H during τ_1 period and of ^{13}C during τ_2 period.

transferred, the remaining 20% being spin-locked, does not evolve, and (ii) the evolution under proton and carbon chemical shift Hamiltonians during τ_1 and τ_2 periods respectively alters the measured dipolar couplings and also has a deleterious effect on the quality of the spectrum due to phase imperfections. These short-comings are addressed in the present work, and modifications are proposed. The modified pulse sequences provide higher sensitivity and are also insensitive to frequency offsets.

Sensitivity Improvement. It is observed that the inclusion of additional aligning pulses to the original pulse sequence shown in Figure 1a improves the sensitivity by 25%. The flip angle and the phase of these pulses can be obtained from the following considerations. The average Hamiltonians corresponding to heteronuclear dipolar coupling with a coupling constant D_{IS} for the pulse sequence shown in Figure 1a during τ_1 and τ_2 are given respectively by eqs 1 and 2 given below.

$$\overline{H}^0_{(1)} = D_{IS}\frac{4}{3\pi}(2I_X + I_Z)S_Z \quad (1)$$

$$\overline{H}^0_{(2)} = D_{IS}\frac{4}{3\pi}(2I_Y + I_Z)S_Z \quad (2)$$

Ideally D_{IS} in the above two equations should be replaced by $(D_{IS} + J_{IS}/2)$ where J_{IS} is the indirect spin−spin coupling between the two spins I and S. In practice J_{IS} may be neglected for carbon−proton systems when the dipolar couplings are of the order of a few kilohertz and the linewidths are a few hundred hertz. The evolution of I_Z magnetization under these Hamiltonians and the $90°_Y$ pulse on the S spin gives rise to S_Y magnetization. In order to make this polarization transfer process efficient, additional pulses on the I spin have been added which are shown in Figure 1b. The flip angle for the pulses to be used has been decided from the following consideration. The Hamiltonian shown in eq 1 takes a simple form when I spin part is transformed by rotation through an angle of 63.4° about the Y axis and is given by

$$\overline{H}^{(0)}_{1_{eff}} = \omega_{IS} 2I_z' S_Z \quad (3)$$

where the prime indicates the operator in the tilted frame. Correspondingly I_Z magnetization transforms into $[I_Z' \cos(\alpha) - I_X' \sin(\alpha)]$. Since only the transverse part of the magnetization evolves under the Hamiltonian shown in eq 3, the intensity of the final signal is proportional to $\sin(63.4°) = 0.89$. The signal can be further enhanced by preparing the initial magnetization I_Z perpendicular to the effective field. To attain this, an initial α° pulse of 26.6° about Y axis is applied as shown in Figure 1b prior to the application of the BLEW-12 pulses. This ensures the transformation of I_Z entirely into I_X'. The evolution of I_X' under the above-mentioned Hamiltonian gives rise to a two spin order term $2I_Y'S_Z \sin(\omega_{IS}\tau_1)$, where ω_{IS} is the scaled dipolar frequency given by $0.47\ D_{IS}$.[20] The scaling of the heteronuclear dipolar coupling is a consequence of the BLEW-12 homonuclear decoupling sequence used during τ_1 and τ_2. The two spin order term gets converted into $2I_Y'\ S_X \sin(\omega_{IS}\tau_1)$ by the application of the 90° pulse on the S spin. Further evolution during τ_2 is visualized by transforming the I spin part to a second frame indicated by double prime, tilted about the X axis. The Hamiltonian shown in eq 2 becomes

$$\overline{H}^{(0)}_{2_{eff}} = \omega_{IS} 2I_z'' S_Z \quad (4)$$

Along with this, $2I'_Y\ S_X$ transforms into

$$2(I_Y'' \cos(\alpha) - I_z'' \sin(\alpha))S_X \quad (5)$$

such that an operator of the type $2I_Z''S_X$ evolving under the Hamiltonian of eq 4 gets converted into S_Y. For an efficient polarization transfer, an α pulse on the I spin about the X axis is applied before the application of the P_{90} block of pulses. The flip angle of this pulse will again be $\alpha = 26.6°$. The modified pulse sequence is shown in Figure 1b. The absence of any one of these pulses reduces the intensity by $\sin\alpha = 0.89°$ and the absence of both reduces the intensity by $\sin^2(\alpha) = 0.8$. The pulse sequence modified for improvement in sensitivity is referred to as DAPT-II.

Elimination of Proton Offset Effects. It is observed that the pulse sequence for DAPT-I shown in Figure 1a is also sensitive to proton and carbon offsets. These offset and chemical-shift dependencies can be eliminated by including refocusing periods as shown in Figure 1c. In this scheme, the evolution of proton magnetization during τ_1 is divided into two equal periods of duration $\tau_1/2$ separated by a 180° pulse applied simultaneously on both I and S, such that evolution under proton offset is refocused while retaining the evolution under the heteronuclear dipolar coupling. During τ_2, S spin chemical shift/offset evolutions can be eliminated in a similar fashion by applying simultaneous π pulses on I and S spins in the middle of the evolution period. Experimentally however the sequence shown in Figure 1c (where the π pulse is applied only on the S spin at $\tau/2$ along with simultaneous commencement of heteronuclear decoupling) was found to perform better.

The pulse sequence with the incorporation of the modification required for both sensitivity enhancement and offset independence is shown in Figure 1c and is henceforth referred to as DAPT-III. The experimental demonstration of the improvements achieved and the use of the pulse sequence for measurement of

heteronuclear dipolar couplings in a liquid crystal are described subsequently.

III. DAPT as PELF and SLF Pulse Sequence

From the discussion in the earlier section, it may be noticed that during τ_1 period an evolution of proton magnetization takes place under heteronuclear dipolar coupling while during τ_2 period a similar evolution of carbon magnetization again under heteronuclear dipolar coupling takes place. This indicates the possibility of using DAPT either as a PELF or as a SLF pulse sequence for obtaining heteronucelar dipolar couplings. As pointed out in the introduction PELF has the advantage of narrower cross-peaks for the dominant dipolar coupling compared to SLF. At the same time proton T_2 is generally shorter than carbon T_2 and this may cause line-broadening in the dipolar dimension in the case of PELF. We compare here the performance of DAPT on a liquid crystalline sample both as a PELF and as a SLF sequence.

IV. Experimental Section

All experiments were performed on a Bruker Avance 500 MHz NMR spectrometer using a 4 mm MAS probe under static condition. The 90° pulse lengths used for ^{1}H and ^{13}C in the experiments were typically 2.9 and 3.0 μs, respectively. The experiments were performed on an oriented nematic liquid crystalline sample of EBBA [*N*-(4-ethoxy benzylidine)-4-*n*-butylaniline] in which a small amount of ^{13}C labeled chloroform was also dissolved. The ^{13}C spectrum of chloroform obtained as a result of polarization transfer from the attached proton by the use of DAPT sequences shown in Figure 1 was used for verifying the proton offset dependence of PELF spectra obtained using DAPT-III. DAPT-III as a PELF and SLF sequence was applied on the liquid crystal sample and the 2D spectra were obtained for the liquid crystal carbons under natural abundance. The PELF spectra were recorded by incrementing τ_1 while τ_2 was kept constant at 139.2 μs which corresponded to four cycles of BLEW-12. Similarly for the SLF experiment, τ_1 was kept constant and τ_2 was varied, as the carbon magnetization evolved. The 2D spectra were recorded typically with 100 t_1 increments and with 8 scans per increment. Prescan delay was kept as 10 s as liquid crystal sample is sensitive to r.f. heating effects. Saturation burst was used in carbon channel so as to cancel the direct carbon magnetization. The two-dimensional data matrix $S(t_1, t_2)$ was subjected to two-dimensional Fourier transformation, using a cosine Fourier transformation in the first time domain. Shifted squared sine-bell function is used while processing. The spectra are plotted in the phase-sensitive mode, after appropriately scaling up the frequency axes to take into account the homonuclear decoupling sequence used (0.47 for BLEW-12, 0.82 for FSLG and 0.57 for PMLG sequence). The maximum t_1 increment for all the 2D experiments were kept nearly as 5.5 ms. In all the cases ^{13}C magnetization was acquired during t_2 with the heteronuclear decoupling sequence SPINAL.[21] For comparison, a PISEMA[5] spectrum of the same sample using the pulse sequence shown in Figure 2 was also obtained under similar experimental conditions as that of DAPT-III. The 2π pulse length for the Lee−Goldburg homonuclear decoupling sequence[22] used during PISEMA was 13.07 μs which corresponded to a proton r.f. power of 62.5 kHz. All experiments were performed with the same acqusition parameters and processed identically. Additionally PISEMA was processed with the qfil option in the Bruker software which uses a Gaussian filter function to remove strong zero frequency peaks in the F_1 dimension[23] while PELF and SLF spectra were processed without qfil.

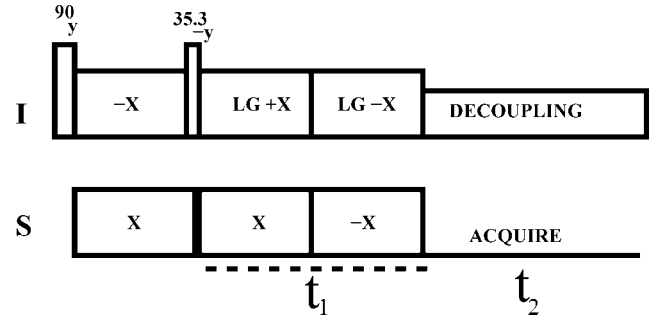

Figure 2. PISEMA pulse sequence.

V. Results and Discussions

Figure 2 is a plot obtained using the SIMPSON[24] simulation program which compares the intensities of the chloroform ^{13}C peak obtained using the DAPT-I and the DAPT-II sequences shown in Figure 1, panels a and b, respectively. Results corresponding to the inclusion of only the initial α° pulse and the inclusion of both the α° pulses are shown. τ_1 is varied over a range of values while τ_2 is kept constant. The inclusion of the two α° pulses in DAPT-II ensures that the magnetization of interest is in a plane perpendicular to direction of the effective field and the entire magnetization takes part in the polarization transfer process. DAPT-II with the two α° pulses shows the maximum intensity and DAPT-I with no aligning pulses gives the least intensity which is 80% of the intensity obtained from DAPT-II. The addition of only one α° pulse at the beginning of the pulse sequence gives an intensity which is higher by approximately 12% compared to the intensity obtained from DAPT-I.

The performance of DAPT-III in terms of its effectiveness for suppression of evolution under proton offsets has been considered. The proton offset was varied systematically over a range of ±5 kHz from the center of the proton spectrum of ^{13}C labeled chloroform and the frequencies of the dipolar oscillations were monitored by incrementing τ_1. The oscillation frequencies were also calculated for this pulse sequence using SIMPSON,[24] for a few selected offsets. Both the experimentally obtained values and the results of simulation indicated that over the selected range of offsets, there was no significant deviation of the measured dipolar coupling. This demostrates that the DAPT-III pulse sequence is able to efficiently refocus the proton chemical shift evolution and provide reliable values of dipolar couplings over a large range of ^{1}H chemical shifts.

The use of DAPT-III as a PELF experiment has been studied by applying it to the liquid crystal EBBA (Figure 3). Spectra were recorded by incrementing τ_1 while τ_2 was kept constant. The obtained 2D data matrix was double Fourier transformed and the resulting spectrum is shown in Figure 3. The F_1 cross-sections corresponding to several carbons are shown in Figure 4. Being a PELF experiment, the extraction of the dipolar couplings from the spectrum is straightforward. The observed splittings in the F_1 dimension in the DAPT spectrum directly provide the dipolar couplings. This is in contrast to SLF experiments based on Hartmann−Hahn cross-polarization[5,7] where the observed splitting in the F_1 dimension corresponds to the proton-carbon dipolar coupling (D_{CH}) only for the methine carbon. For the methylene carbon the splitting corresponds to $\sqrt{2}\ D_{CH}$. For the methyl carbon there are three peaks corre-

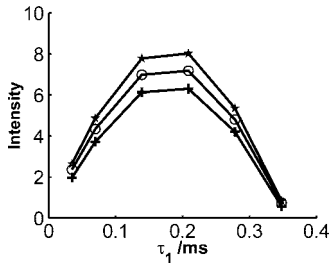

Figure 3. Plot of S spin intensity corresponding to DAPT-II pulse sequence obtained from simulation as a function of τ_1 to show the effect of inclusion of initial 26° pulses for aligning magnetization. (+) No initial pulses, (○) with the inclusion of one pulse, and (∗) with the inclusion of both the pulses.

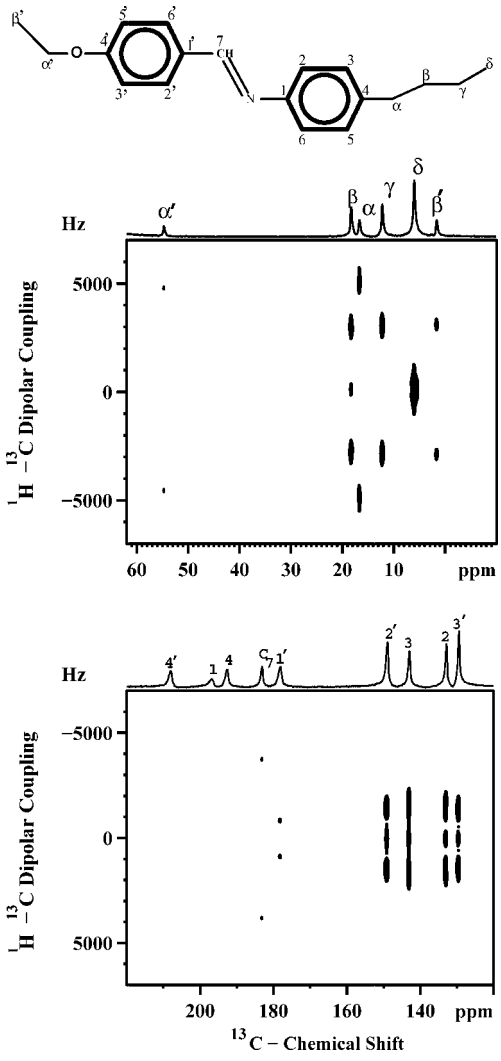

Figure 4. PELF spectrum of the liquid crystal EBBA obtained using the DAPT-III pulse sequence shown in Figure 1c by incrementing τ_1 as t_1. The aliphatic and the aromatic parts of the spectra are shown separately.

TABLE 1: ^{1}H−^{13}C Dipolar Couplings (D_{CH}) Obtained for the Liquid Crystal EBBA by Using the DAPT Sequence as a PELF Experiment

carbon labels	α	β	γ	α′	β′	7	2	3	2′	3′
D_{CH} (kHz)	4.9	2.9	2.9	4.7	3.0	3.8	1.7	1.9	1.5	1.4

sponding to D_{CH}, $\sqrt{3}$ D_{CH}, and $2D_{CH}$.[25] So also for the aromatic carbons the observed splitting has contributions from the directly bonded proton as well as from the proton at the ortho position.[26]

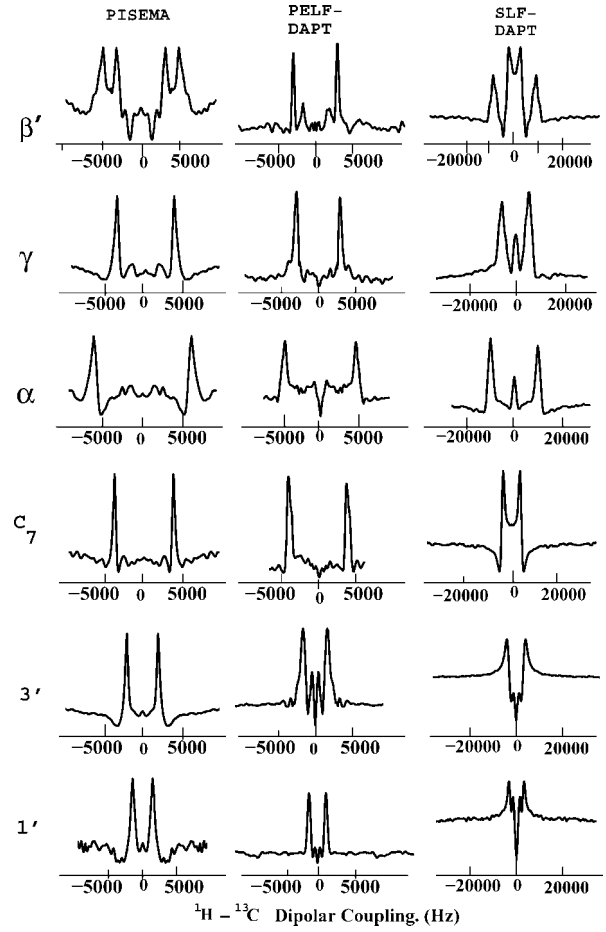

Figure 5. Cross-sections corresponding to several carbon resonances from three different 2D experiments. The first, second and third columns correspond respectively to PISEMA, DAPT-PELF, and DAPT-SLF experiments. The horizontal scale for the DAPT-SLF plot has been approximately four times larger than the other two, to accommodate the larger spectral window in this case.

Hence the extraction of the dipolar coupling in this case is not straightforward. The measured dipolar couplings from the spectrum shown in Figure 4 are summarized in Table 1 for various carbons. These couplings provide useful information about order and dynamics in the liquid crystal. For example, the order parameter of the long axis of the molecule is obtained from the dipolar coupling of the C_7 carbon using

$$D_{CH} = \frac{\gamma_H \gamma_C}{4\pi r^3} S \frac{(3\cos^2\theta - 1)}{2} \qquad (6)$$

where $\gamma_H\gamma_C/4\pi r^3 = 22.68$ kHz for the case of a proton directly bonded to a carbon, S is the order parameter of the long axis of the liquid crystal molecule, and θ is the angle between the CH vector and the long axis. As reported in earlier studies,[26] the $C_1{\cdot}C_7H$ bond angle was taken to be 114° and assuming a tilt of 3.5° between the $C_1{\cdot}C_7$ bond and the long axis, the order parameter S turns out to be 0.54. Application of eq 6 to the aromatic protonated carbons gives an angle of 60° ± 1° for the long axis of the molecule with respect to the CH vectors which indicates that the long axis of the molecule is nearly parallel to the para axis of both the benzene rings of EBBA. The dipolar couplings of α, β, γ, α′, and β′ carbon provide local order parameter obtained as D_{CH}/22.68 kHz, which are respectively 0.22, 0.13, 0.13, 0.21, and 0.13. These are in general agreement with values reported earlier.[26]

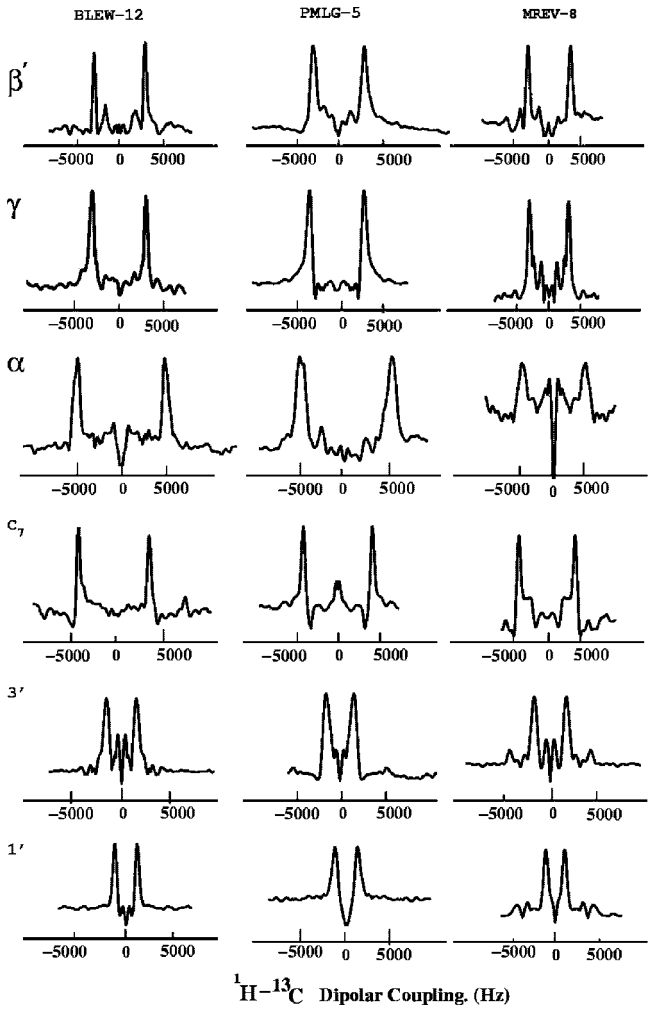

Figure 6. Cross-sections corresponding to several carbon resonances of EBBA obtained from the 2D spectra employing either BLEW-12 or PMLG-5 or MREV-8 for homonucelar decoupling in the DAPT sequence. The frequency axes of the spectra have been appropriately scaled up taking into account the homonuclear decoupling sequence employed (vide text).

Use of DAPT as an SLF experiment has also been explored. The result of this experiment along with PISEMA and DAPT as a PELF experiment is presented in Figure 4. Typical cross-sections of different types of carbons are shown in this figure. In the case of DAPT-SLF experiment, the dipolar evolution for a CH carbon results in a doublet with a separation equal to $2D_{CH}$. The CH_2 carbon also provides a doublet but with a separation $4D_{CH}$. The CH_3 carbon results in two doublets, the inner doublet having a separation equal to $2D_{CH}$ and the outer doublet having a separation equal to $6D_{CH}$. In contrast, the DAPT-PELF experiment results in a doublet of splitting $2D_{CH}$ for all the three types of carbons. As mentioned earlier PISEMA experiment results in a doublet of splitting $2D_{CH}$ and $2\sqrt{2}\ D_{CH}$ for the methine and the methylene carbons respectively while the methyl carbon gives rise to three doublets with the doublet splitting being $2D_{CH}$, $2\sqrt{3}\ D_{CH}$, and $4D_{CH}$. Therefore, DAPT-SLF experiment requires the largest spectral window in the F_1 dimension. This is seen in the cross-sections shown in Figure 4. For the C_7 carbon, the doublet spacings obtained from the three experiments are nearly the same. For the methylene C_γ carbon, the PELF experiment has the smallest splitting (2.8 kHz) with the PISEMA (3.7 kHz) and SLF (6.0 kHz) experiments showing increasingly larger splittings as anticipated. It also turns out that the line-width of the cross-peaks in the F_1 dimension is the smallest in the case of PELF. For example in the case of C_γ carbon the line-width for PELF, PISEMA, and SLF experiments are 500, 600, and 2000 Hz, respectively. This is as expected since in the PELF experiment the proton evolution in unlabeled samples takes place under a single proton-carbon coupling. In contrast in SLF, the evolution of the carbon magnetization takes place under heteronuclear dipolar couplings of the carbon not only to the bonded proton but also to the remote protons. Therefore the lines are relatively broader compared to the lines obtains with PELF. Between PISEMA and SLF, PISEMA provides narrower lines as the smaller couplings are truncated in the presence large couplings.[25] The advantage of the use of DAPT-PELF is most obvious in the case of the methyl (β') carbon. While SLF and PISEMA provide multiple sets of overlapping doublets, DAPT-PELF provides a single pair of sharp well-resolved lines, making accurate measurement of dipolar coupling easier. So also for the case of the protonated aromatic carbon 3′, the one bond coupling is directly obtained from the PELF spectrum.

We have also investigated the use of homonuclear decoupling sequences, besides BLEW-12, in DAPT such as PMLG-5[27] and MREV8.[28] The results with these three sequences from the DAPT-PELF experiment on a sample of EBBA are shown in Figure 5 where cross-sections corresponding to different carbons of EBBA are given. PMLG has a slightly higher scaling factor of 0.57 compared to 0.47 for BLEW-12 and MREV-8. This should be an advantage provided the line width remains small. It has been documented earlier that the decoupling efficiency of PMLG is indeed assisted by MAS.[29] The relatively poor performance of PMLG in static case is borne out in Figure 5 with PMLG-5 yielding line widths that are larger than those provided by either BLEW-12 or MREV-8. The latter two sequences are comparable in performance which is as expected as both are ideally designed for static cases.

VI. Conclusions

We have demonstrated the use of the newly proposed heteronuclear polarization transfer scheme, namely DAPT, for separated local field spectroscopy. A liquid crystal sample at natural abundance has been used as a test sample for carrying out the experiments. The DAPT sequence proposed earlier has been improved by incorporating modifications for sensitivity enhancement and for offset compensation. The improved sequence referred to as DAPT-III has been implemented both as a proton evolution and also as a carbon evolution technique and the relative performances have been compared. In the case of DAPT implemented as a SLF technique, the carbon evolution takes place in the presence of short-range as well as long-range proton−carbon dipolar couplings. Depending upon the number of protons attached to the carbon, the frequency measured in the F_1 dimension varies. Further unresolved long-range couplings contribute to broadening of the dipolar cross-peaks. Similar problems are encountered in the case of PISEMA also. But in the case of DAPT-PELF, carbon being a rare spin proton magnetization evolution sees only one coupled carbon. Therefore the experiment gives directly the dipolar coupling between the carbon and the attached proton. Experimental results presented in this paper are in conformity with the above observations and indicate that DAPT-PELF is a better 2D technique for resolving chemical shifts and dipolar couplings. It may be mentioned that the DAPT method has other advantages in comparison to techniques based on Hartmann−Hahn cross-polarization. These are (i) for implementation of DAPT no r.f. matching condition needs to be satisfied and (ii) the r.f. power used for polarization

transfer on the S spin is minimal, just one $\pi/2$ pulse, which should help in minimizing the heating effect on the sample. In conclusion DAPT-PELF could be an useful alternative for existing SLF experiments for the study of structure and dynamics of oriented liquid crystalline and biological samples. It may be mentioned that long-range proton-carbon dipolar couplings appear in PELF spectra as separate doublets close to the center of the spectra.[30] We have observed such couplings in some liquid crystal systems. These couplings are useful since they provide valuable structural correlation and efforts to utilize such information for novel liquid crystalline systems are underway.

References and Notes

(1) Hester, R. K.; Ackerman, J. L.; Neff, B. L.; Waugh, J. S. *Phys. Rev. Lett.* **1976**, *36*, 1081.

(2) Ramamoorthy, A.; Wei, Y. F.; Lee, D. K. *Annu. Rep. NMR Spectrosc.* **2004**, *52*, 1.

(3) Hartmann, S. R.; Hahn, E. L. *Phys. Rev.* **1962**, *128*, 2042.

(4) Muller, L.; Kumar, A.; Ernst, R. R. *Phys. Rev. Lett.* **1974**, *32*, 1402.

(5) Wu, C. H.; Ramamoorthy, A.; Opella, S. J. *J. Magn. Reson. A* **1994**, *109*, 270.

(6) Ramamoorthy, A.; Wu, C. H.; Opella, S. J. *J. Magn. Reson.* **1999**, *140*, 131.

(7) Pratima, R.; Ramanathan, K. V. *J. Magn. Reson.* **1996**, *118*, 7.

(8) Nevzorov, A. A.; Opella, S. J. *J. Magn. Reson.* **2003**, *164*, 182.

(9) Nishimura, K.; Naito, A. *Chem. Phys. Lett.* **2005**, *402*, 245.

(10) Nishimura, K.; Naito, A. *Chem. Phys. Lett.* **2006**, *419*, 120.

(11) Dvinskikh, S. V.; Yamamoto, K.; Ramamoorthy, A. *J. Chem. Phys.* **2006**, *125*, 034507.

(12) Nakai, T.; Terao, T. *Magn. Reson. Chem.* **1992**, *30*, 42.

(13) Schmidt-Rohr, K.; Nanz, D.; Emsley, L.; Pines, A. *J. Phys. Chem.* **1994**, *98*, 6668.

(14) Hong, M.; Pines, A.; Calderalli, S. *J. Phys. Chem.* **1996**, *100*, 14815.

(15) Fung, B. M.; Ermolaev, K.; Yu, Y. *J. Magn. Reson.* **1999**, *138*, 28.

(16) Calderalli, S., *Encyclopedia of NMR*; Grant, D. M., Harris, R. K., Eds.; John Wiley: Chichester, U.K., 2002; Vol. 9, p 291.

(17) Jayanthi, S.; Madhu, P. K.; Kurur, N. D.; Ramanathan, K. V. *Chem. Phys. Lett.* **2007**, *439*, 407.

(18) Morris, G. A.; Freeman, R. *J. Am. Chem. Soc.* **1979**, *101*, 760.

(19) Zhao, X.; Hoffbauer, W.; Schmedt auf der Günne, J.; Levitt, M. H. *Solid State Nucl. Magn. Reson.* **2004**, *26*, 57.

(20) Burum, D. P.; Linder, M.; Ernst, R. R. *J. Magn. Reson.* **1981**, *44*, 173.

(21) Fung, B. M.; Khitrin, A. K.; Ermolaev, K. *J. Magn. Reson.* **1981**, *142*, 97.

(22) Lee, M.; Goldburg, W. I. *Phys. Rev. A* **1965**, *140*, 1261.

(23) Marion, D.; Ikura, M.; Bax, A. *J. Magn. Reson.* **1989**, *84*, 425.

(24) Bak, M.; Rasmussen, J. T.; Nielsen, N. C. *J. Magn. Reson.* **2000**, *147*, 296.

(25) Gan, Z. *J. Magn. Reson.* **2000**, *143*, 136.

(26) Nagaraja, C. S.; Ramanathan, K. V. *Liq. Cryst.* **1999**, *26*, 17.

(27) Vinogradov, E.; Madhu, P. K.; Vega, S. *Chem. Phys. Lett.* **1999**, *314*, 443.

(28) Rhim, W. K.; Elleman, D. D. *J. Chem. Phys.* **1973**, *59*, 3740.

(29) Vinogradov, E.; Madhu, P. K.; Vega, S. *Top. Curr. Chem.* **2005**, *246*, 33.

(30) Caldarelli, S.; Hong, M.; Emsley, L.; Pines, A. *J. Phys. Chem.* **1996**, *100*, 18696.

JP804764Q